

# The oxidation of 6-hydroxydopamine in aqueous solution. Part 3.<sup>12</sup> Kinetics and mechanism of the oxidation with iron(III)†

2 PERKIN

Guy N. L. Jameson\*‡ and Wolfgang Linert

Institute of Inorganic Chemistry, Technical University of Vienna, Getreidemarkt 9/153, A-1060, Vienna, Austria. E-mail: gjameson@physics.emory.edu; wlinert@mail.zserv.tuwien.ac.at

Received (in Cambridge, UK) 5th September 2000, Accepted 15th February 2001

First published as an Advance Article on the web 20th March 2001

The kinetics of the oxidation of 6-hydroxydopamine [5-(2-aminoethyl)benzene-1,2,4-triol, protonated form H<sub>3</sub>LH<sup>+</sup>] by iron(III) under anaerobic conditions are presented. A complex mechanism whereby the *o*- (*o*Q), *p*- (*p*Q), and triketo-quinones (tQ) are formed *via* parallel inner- and outer-sphere electron transfer mechanisms has been established. The outer-sphere mechanism is particularly fast (nearly diffusion limiting) and predominates. By following the dependence of the rate on ionic strength it has been shown that a deprotonated form of 6-hydroxydopamine reacts *via* an outer-sphere reaction with all species of iron. Like the other catecholamines [3,4-dihydroxy-1-(2-aminoethyl)benzenes], but to a much smaller extent, complex formation occurs by FeOH<sup>2+</sup> reacting with the fully protonated form of 6-hydroxydopamine. Three different semiquinones are initially produced; two of them, the triketo- and *p*-semiquinones, are tautomers. The *o*- and triketo-semiquinones react quickly with another iron atom to form their respective quinones. The *p*-semiquinone, however, is seemingly stable, partly reacting with more iron and partly disproportionating to form *p*Q and reforming 6-hydroxydopamine. At pHs above 2.5, *p*Q and *o*Q are in equilibrium *via* a deprotonated quinone Q<sup>-</sup>. The biological implications of this mechanism are discussed.

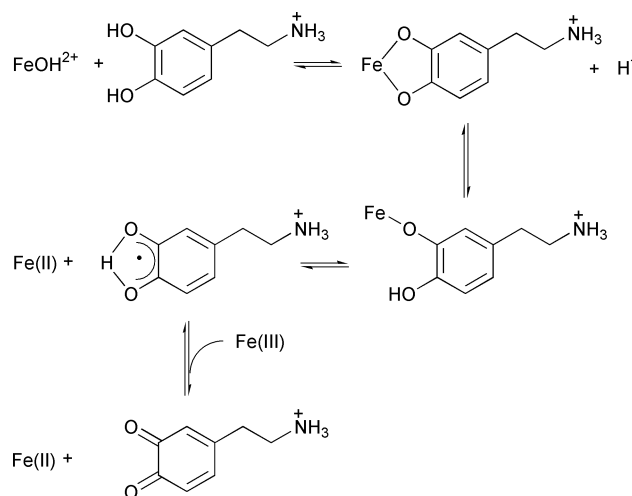
## Introduction

The reduction of iron(III) by 6-hydroxydopamine (protonated form, H<sub>3</sub>LH<sup>+</sup>) is of considerable biological interest because it provides a possible mechanism for the release of iron from ferritin during the progression of Parkinson's disease.<sup>1</sup> However, the potentially simpler but important kinetics of the reaction of 6-hydroxydopamine with aqueous iron(III) have until now not been investigated.

In general, catecholamines<sup>2,3</sup> react only at low pH (0–3) with iron(III). At higher pHs bis- and tris-complexes are formed, which are relatively stable towards internal electron transfer, probably due to the catecholamine acting as a non-innocent ligand. The mono-chelate complexes, which absorb at around 700 nm, protonate to form mono-dentate complexes, which all undergo internal electron transfer to form the respective semiquinone and release iron(II). These semiquinones are unstable and react immediately with another iron(III), see Scheme 1. Note that excess iron(II) reverses all these reactions to re-produce the green complex.

Noradrenaline,<sup>4</sup> however, is seen to react *via* two parallel pathways, the major one involving complex formation, and the other involving direct electron transfer. (The latter is only observed when noradrenaline is present in relatively low concentrations.) Similarly, at low pH, there is no evidence for a complex between 6-hydroxydopamine and iron(III). It is therefore believed that a similar mechanism is operating.

The kinetics of 6-hydroxydopamine oxidation are, however, particularly difficult to interpret because of the complicated product speciation. Depending on the pH, up to four different quinones are produced by the two, one-electron transfers to



**Scheme 1** The oxidation of dopamine at low pH by iron(III) *via* complex formation.

iron(III)—the *p*- (*p*Q), *o*- (*o*Q), triketo- (*t*Q) and the deprotonated-quinone (Q<sup>-</sup>) (see Parts 1 and 2).

6-Hydroxydopamine and its various quinones absorb in the UV–Vis region of the electronic spectrum making them suitable for study by stopped-flow spectroscopy. Unfortunately, 6-hydroxydopamine is photolysed when exposed to light of a wavelength less than approximately 300 nm producing unknown products that also absorb in this region. However, as was shown in Part 2, because 6-hydroxydopamine is in excess this reaction could be corrected for by subtraction of an appropriate linear absorption–time curve. Another complication is that *p*Q and *t*Q have strongly overlapping absorptions with an envelope maximum at 265 nm. Both species were therefore followed together until a pH of 2.5, at which point only *p*Q is formed. The previous part reports the molar absorbances of all the species and a study of the product speciation. This

† Rate constants and absorbance data are available as supplementary data. For direct electronic access see <http://www.rsc.org/suppdata/p2/b0/b007203f/>

‡ Present address: Department of Physics, Rollins Research Center, Emory University, Atlanta, GA 30322, USA.

§ For convenience, –OH protons are written to the left, and the –NH<sub>3</sub><sup>+</sup> proton to the right of L.

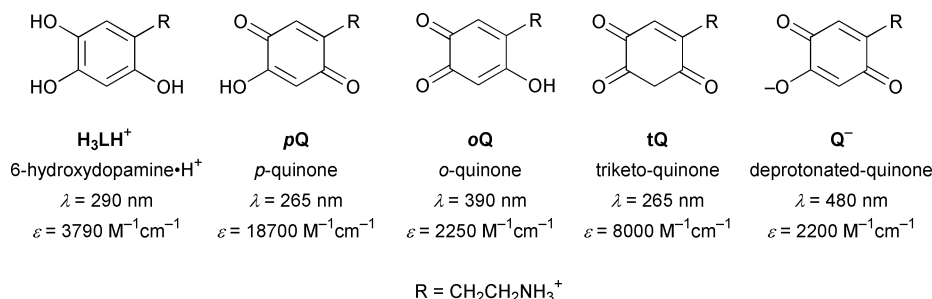


**Fig. 1** The structures and optical properties of the species investigated. (Note that the maxima quoted for *pQ* and *tQ* refer to the maximum of the absorption envelope and not those of the individual quinones, see Part 2.)

information, some of which is presented in Fig. 1, is utilised in the present pH-dependent kinetic studies.

## Experimental

### (i) Chemicals

The 6-hydroxydopamine used came from two sources, Sigma-Aldrich and Fluka. Iron(III) was in the form of  $\text{Fe}(\text{NO}_3)_3 \cdot 9\text{H}_2\text{O}$  as supplied by Fluka (*pro analysi*).

### (ii) pH Meter

A Radiometer pH meter (pHM84) was used with pH electrodes from Cole-Palmer, Radiometer, and Hamilton. Initial calibration was carried out using two buffers (pH 2.00 and 7.00) obtained from either Riedle-de Haën or Merck. Further calibration of the results was achieved by using the formula established by Gorton.<sup>5</sup> The formula,  $\text{pH}_{\text{corr}} = \text{pH} - \{0.131/(0.984\text{pH})\}$  was verified by titrating various concentrations of nitric acid in 0.1 M solutions of  $\text{KNO}_3$ .

### (iii) Stopped-flow

A stopped-flow system from Applied Photo-Physics was used (SX-17MV) with PEEK valves and flow system to minimise the entry of oxygen during runs. The flow system was prepared at the beginning of each day by purging for one hour with a 0.25 M sodium dithionite solution.

Data collection and initial manipulation were carried out on an Acorn 5000 computer using Applied Photo-Physics' own software. Further manipulation of the data was carried out employing Excel on a PC.

6-Hydroxydopamine was always in at least a five-fold excess over iron(III) in order to achieve pseudo-(first)-order kinetics. The range of concentrations used was: for 6-hydroxydopamine 0.30–4.00 mM; and for iron(III) 0.02–0.80 mM. The ionic strength was maintained at 0.1 M with  $\text{KNO}_3$  (except when ionic strength dependencies were measured). All solutions were purged with argon and then transferred to the stopped-flow apparatus in gas-tight Hamilton syringes in order to exclude oxygen.

## Results and discussion

### Kinetics at low pH

As stated above, at low pH no complex was observed. The formation of *oQ* was found to obey an accurate first-order relationship (*i.e.*  $d[\text{oQ}]/dt = k_{\text{obs}}[\text{oQ}]$ ), see Fig. 2. Although the sum of *pQ* and *tQ* did not follow such a rate law over the complete time-scale, it was found that the first part of the absorption–time curve could also be fitted to a first-order rate law (see Fig. 2). (The deviation towards the end of the reaction is consistent with a second-order rate law, see below.)

A plot of  $\log(k_{\text{obs}}/[\text{L}]_T)$  vs. pH for all species, including  $\text{Q}^-$  and 6-hydroxydopamine itself, is given in Fig. 3. (The formation of the deprotonated quinone,  $\text{Q}^-$  is discussed below.) The fitted curve relies on data for *oQ* alone at low pH because

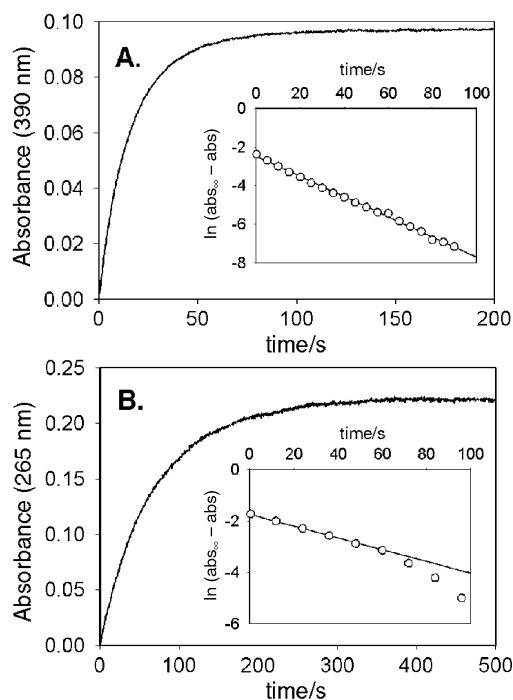


**Fig. 2** A. The formation of *oQ* is first-order. ( $[\text{L}] = 1.52 \text{ mM}$ ;  $[\text{Fe}]_{\text{added}} = 0.255 \text{ mM}$ ;  $\text{pH} = 1.02$ .) B. The formation of (*pQ* + *tQ*) is only first-order over about one half-life under these conditions. ( $[\text{L}] = 0.379 \text{ mM}$ ;  $[\text{Fe}]_{\text{added}} = 0.0409 \text{ mM}$ ;  $\text{pH} = 1.13$ .)

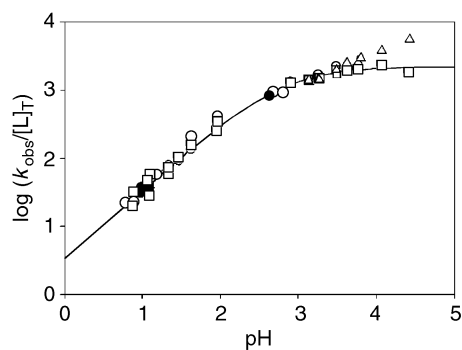


**Fig. 3**  $\log(k_{\text{obs}}/[\text{L}]_T)$  vs. pH where  $k_{\text{obs}}$  is the initial first-order rate constant (typical results). The fitted curve relies on data for *oQ* alone at low pH (see text).  $\circ = \text{oQ}$ ;  $\square = (\text{pQ} + \text{tQ})$ ;  $\triangle = \text{Q}^-$ ;  $\bullet = \text{L}$ .

this is the only species that is accurately first-order over the whole time-scale and can be followed without the interference of photolysis—see Part 2.

It can be seen that all species (the appearance of *oQ* and (*pQ* + *tQ*); and the disappearance of 6-hydroxydopamine) have the same initial rate at low pH. This shows that they are, in fact, all following the disappearance of iron *i.e.* that this is the rate-determining step. At low pH (1–2) the reaction is reciprocal first-order in protons. For most catecholamines<sup>2,3</sup> this proton dependence is caused by the iron speciation and was

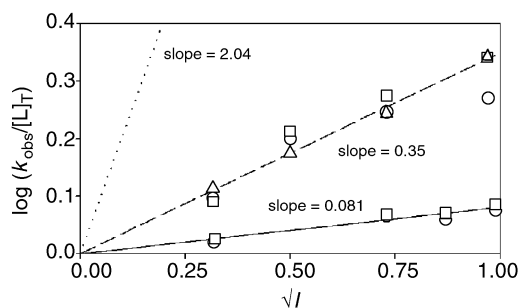


**Fig. 4** The ionic strength dependence of  $k_{\text{obs}}$  at two pHs.  $\circ = oQ$ ,  $\square = (pQ + tQ)$ ,  $\triangle = Q^-$  — = pH 1.07, — — = pH 3.50, ..... = theoretical slope observed for dopamine.

explained by  $[\text{Fe}(\text{OH})]^{2+}$  reacting exclusively with the fully protonated ligand, thus enabling an accurate value for the protonation constant of  $[\text{Fe}(\text{OH})]^{2+}$  ( $K^{\text{FeOH}} = 660 \text{ M}^{-1}$ ) to be obtained. When this relationship was used to fit the data obtained in this study, however, a good fit was only possible over a very short pH range. An alternative explanation was therefore sought.

#### Ionic strength dependence

The relationship shown in eqn. (1) exists between rate constants and ionic strength<sup>6</sup> in which  $I = \frac{1}{2} \sum z_i^2 m_i$ ;  $z_i$  is the charge number of an ion  $i$  and  $m_i$  is its molality;  $\dagger A = 0.509 (\text{mol kg}^{-1})^{-\frac{1}{2}}$  for aqueous solutions.

$$\log \left( \frac{k_{\text{rxn}}}{k_{\text{rxn}}^0} \right) = 2Az_+z_-I^{\frac{1}{2}} \quad (1)$$

If, therefore,  $\log(k_{\text{rxn}}/k_{\text{rxn}}^0)$  is plotted vs.  $I^{\frac{1}{2}}$  then the slope will give a measure of the product of the charges of the reacting species. The gradient of such a plot for dopamine,<sup>2</sup> which reacts solely *via* a complex, was found to be 2. This is effectively the theoretical slope (2.04) for the reaction between a doubly charged species with a singly charged one. The data were therefore consistent with a reaction between  $[\text{Fe}(\text{OH})]^{2+}$  and  $\text{H}_2\text{LH}^+$ .

However, 6-hydroxydopamine is found to have a near zero ionic strength dependence at pHs of 1.07 and 3.53 (see Fig. 4) and this is consistent with a reaction between all forms of iron with the deprotonated ligand ( $\text{H}_2\text{LH}$ ) which has an overall charge of zero [eqn. (2)].

$$-\frac{d[\text{Fe}]}{dt} = k_{\text{rxn}}[\text{Fe}]_{\text{T}}[\text{H}_2\text{LH}] \quad (2)$$

This is, of course, assuming that the rate constants are nearly the same for both iron species involved (*i.e.* both  $\text{Fe}^{3+}$  and  $[\text{Fe}(\text{OH})]^{2+}$ ).

The slight positive dependence implies that, whereas noradrenaline<sup>4</sup> reacts mainly by complex formation with a small contribution of an outer-sphere reaction, 6-hydroxydopamine reacts mainly by the outer-sphere reaction with a small contribution from that proceeding *via* complex formation. Furthermore, the slope measured at a pH of 3.53 is slightly more positive than at a pH of 1.07 (0.35 compared with 0.081), and this adds to the expectation that the reaction *via* complex formation will increase in importance as the pH is increased. This is confirmed when both the concentrations and the pH are high and a small amount of a complex between iron(III) and 6-hydroxydopamine (which then very rapidly disappears) can be observed at 720 nm (see Fig. 5).

<sup>†</sup> Note that molalities should in fact be used, but the error introduced by using molarities is not large. However, deviations should be expected at high values of  $I$ , because the Debye–Hückel limiting law is no longer valid.

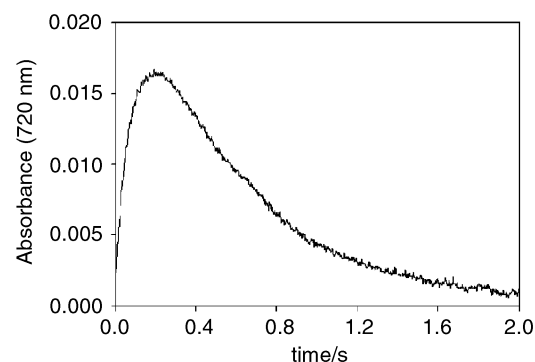


**Fig. 5** Evidence for the existence of a complex between 6-hydroxydopamine and iron(III). ( $[\text{L}] = 1.06 \text{ mM}$ ;  $[\text{Fe}]_{\text{added}} = 0.185 \text{ mM}$ ;  $\text{pH} = 3.53$ .)

#### Limiting value of the rate

A protonation constant<sup>||</sup> can be expressed as the ratio of the rates of the protonation and deprotonation reactions *e.g.* the last protonation constant of 6-hydroxydopamine,  $K_4$  is given by eqn. (3).

$$K_4 = \frac{[\text{H}_3\text{LH}^+]}{[\text{H}_2\text{LH}][\text{H}^+]} = \frac{k_+}{k_-} = 10^{8.88} \quad (3)$$

*Protonation reactions* are almost always fast and in fact nearly diffusion limited *i.e.*  $k_+ \approx 10^{11} \text{ M}^{-1} \text{ s}^{-1}$ . This means that because the final protonation of 6-hydroxydopamine is very high ( $K_4 = 10^{8.88} \text{ M}^{-1}$ )  $k_-$  must be very slow *i.e.*  $k_- \approx 10^2 \text{ s}^{-1}$ . This has important consequences because it means that any reaction of  $\text{H}_2\text{LH}$  must be limited by the rate of deprotonation of  $\text{H}_3\text{LH}^+$ . The formation of the deprotonated 6-hydroxydopamine,  $\text{H}_2\text{LH}$ , can therefore be treated as a Bodenstein intermediate, where  $k_{\text{rxn}}$  is the sum of all the rate constants referring to the disappearance of iron, giving eqn. (4). This leads to eqn. (5).

$$\frac{d[\text{H}_2\text{LH}]}{dt} = 0 = k_-[\text{H}_3\text{LH}^+] - k_+[\text{H}_2\text{LH}][\text{H}^+] - k_{\text{rxn}}[\text{H}_2\text{LH}][\text{Fe}]_{\text{T}} \quad (4)$$

$$[\text{H}_2\text{LH}] = \frac{[\text{H}_3\text{LH}^+]}{\{K_4[\text{H}^+] + (k_{\text{rxn}}[\text{Fe}]_{\text{T}}/k_-)\}} \quad (5)$$

At all pH values below about 7,  $[\text{H}_3\text{LH}^+] = [\text{L}]_{\text{T}}$  and hence eqn. (6) applies. The factor 2 appears because the formation of one quinone requires two iron(III) ions.

Reaction rate =

$$2k_{\text{rxn}}[\text{H}_2\text{LH}][\text{Fe}]_{\text{T}} = \frac{2k_{\text{rxn}}[\text{Fe}]_{\text{T}}[\text{L}]_{\text{T}}}{\{K_4[\text{H}^+] + (k_{\text{rxn}}[\text{Fe}]_{\text{T}}/k_-)\}} \quad (6)$$

It can furthermore be seen that when  $[\text{H}^+]$  is very low (*i.e.* pH is high)  $K_4[\text{H}^+] \ll (k_{\text{rxn}}[\text{Fe}]_{\text{T}}/k_-)$  so that eqn. (7) is true. Note that this means that the rate is also eventually zero-order in iron.

$$\left. \frac{k_{\text{obs}}}{[\text{L}]_{\text{T}}} \right|_{\text{lim}[\text{H}^+] \rightarrow 0} = 2k_- \quad (7)$$

Fig. 3 (see also Fig. 6) indeed shows that  $k_{\text{obs}}/[\text{L}]_{\text{T}}$  for  $pQ$  reaches a limit of  $2200 \text{ M}^{-2} \text{ s}^{-1}$  at high pH (paradoxically,  $Q^-$  does increase above this value for reasons explained below). This value of  $1100 \text{ M}^{-2} \text{ s}^{-1}$  seems a little high because it implies

<sup>||</sup> Protonation constants are used throughout this work in line with compilations of data, and to be consistent with metal complex formation constants.

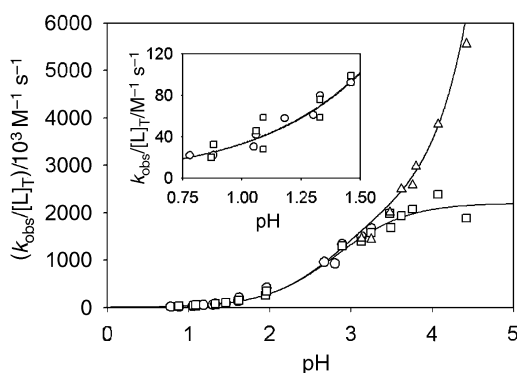


**Fig. 6** Plot of  $k_{\text{obs}}/[L]_{\text{T}}$  vs. pH showing the limiting rate for oxidation to  $pQ$  and deviation from this by the  $Q^-$  (see text) ( $\circ = oQ$ ;  $\square = (pQ + tQ)$ ;  $\triangle = Q^-$ ).

that  $k_+$  is  $8.34 \times 10^{11} \text{ M}^{-1} \text{ s}^{-1}$  and this is faster than the accepted rate of transfer of a proton in water.<sup>7</sup> This could, however, be explained by the first deprotonation constant referring to the deprotonation of one of the two *o*-hydroxy groups, thus providing a statistical factor of two.  $k_-$  is, therefore, effectively about  $550 \text{ M}^{-1} \text{ s}^{-1}$ . The product of the deprotonation is almost certainly internally hydrogen bonded thereby making  $k_-$  more favourable but even allowing for these effects the value remains inexplicably high.

At low pH the expression for the rate of reaction [eqn. (6)] is given in eqn. (8).

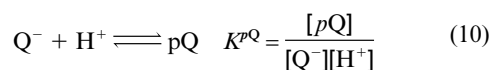
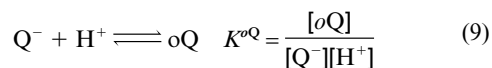
$$\text{Reaction rate} = 2k_{\text{rxn}}[\text{H}_2\text{LH}][\text{Fe}]_{\text{T}} = \frac{2k_{\text{rxn}}[\text{Fe}]_{\text{T}}[\text{L}]_{\text{T}}}{K_4[\text{H}^+]} \quad (8)$$

This is reciprocal first-order in  $[\text{H}^+]$  as is in fact observed. A plot of  $k_{\text{obs}}/[L]_{\text{T}}$  vs.  $1/[\text{H}^+]$  thus enables  $k_{\text{rxn}}$  to be calculated. A value of  $1.34 \pm 0.05 \times 10^9 \text{ M}^{-1} \text{ s}^{-1}$  was obtained. Note that the same result is obtained from the intercept in Fig. 3.

Over a relatively short intermediate pH range (which, naturally, also depends upon the initial iron(III) concentration) the rate with respect to  $[\text{Fe}]_{\text{T}}$  is neither first-order nor zero-order. But, for reactions carried out under pseudo-order conditions, the rate is independent of the concentration of the reactant not in excess whether it has a first- or a zero-order dependence. Thus the values of  $k_{\text{obs}}/[L]_{\text{T}}$  are continuous with respect to change in pH. (Following the disappearance of iron directly would, of course, show a change in order but this is unfortunately impossible using this technique.)

### Deprotonation of the quinones

It can be seen from Figs. 3 and 6 that the rate of formation of  $Q^-$ , unlike that of  $pQ$ , and contrary to expectations, does not seem to be limited by the rate of deprotonation of the 6-hydroxydopamine. However, this paradox is readily explained because  $pQ$ ,  $oQ$  and  $Q^-$  are in equilibrium above a pH of about 2.5 [eqns. (9) and (10), rearranging gives eqn. (11)].



$$[Q^-] = \frac{[oQ]}{K^{oQ}[\text{H}^+]} = \frac{[pQ]}{K^{pQ}[\text{H}^+]} \quad (11)$$

Differentiating yields eqn. (12), which can be rearranged to eqn. (13).

$$\frac{d[Q^-]}{dt} = \frac{1}{K^{oQ}[\text{H}^+]} \times \frac{d[oQ]}{dt} = \frac{1}{K^{pQ}[\text{H}^+]} \times \frac{d[pQ]}{dt} \quad (12)$$

$$\frac{d[oQ]}{dt} = \frac{K^{oQ}}{K^{pQ}} \times \frac{d[pQ]}{dt} \quad (13)$$

Over this pH range,  $oQ$  cannot be measured reliably because the broad band at 480 nm (corresponding to  $Q^-$ ) swamps its small contribution at 390 nm and so only  $pQ$  data can be used. At equilibrium the rate of appearance of the sum of  $pQ$  and  $Q^-$  now equals half the rate of disappearance of iron (the rate-determining step), eqn. (14).

$$\begin{aligned} -\frac{d[\text{Fe}]_{\text{T}}}{dt} &= 2 \left\{ \frac{d[pQ]}{dt} + \frac{d[Q^-]}{dt} \right\} \\ &= 2 \frac{d[pQ]}{dt} \left\{ 1 + \frac{1}{K^{pQ}[\text{H}^+]} \right\} \\ &= \frac{2(k_1 + k_2)[\text{Fe}]_{\text{T}}[\text{L}]_{\text{T}}}{\{K_4[\text{H}^+] + (k_1 + k_2)[\text{Fe}]_{\text{T}}/k_-\}} \left\{ 1 + \frac{1}{K^{pQ}[\text{H}^+]} \right\} \quad (14) \end{aligned}$$

At  $\text{pH} > 3.5$ ,  $K_4[\text{H}^+] \ll (k_1 + k_2)[\text{Fe}]_{\text{T}}/k_-$ . Hence eqn. (15) may be derived.

$$-\frac{d[\text{Fe}]_{\text{T}}}{dt} = 2k_-[\text{L}]_{\text{T}} \left\{ 1 + \frac{1}{K^{pQ}[\text{H}^+]} \right\} \quad (15)$$

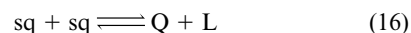
This shows that now the rate of formation of  $Q^-$  can paradoxically exceed the limit set by deprotonation of 6-hydroxydopamine by virtue of the deprotonation reactions of the quinones. All the data can now be plotted with appropriate theoretical lines—see Fig. 6.

### Second-order component of the reaction

As shown above, the appearance of neither  $pQ$  nor  $Q^-$  is first-order over the whole time-scale. In fact, towards the end of the reaction, they both follow a rate equation corresponding to a second-order reaction (see Fig. 7).

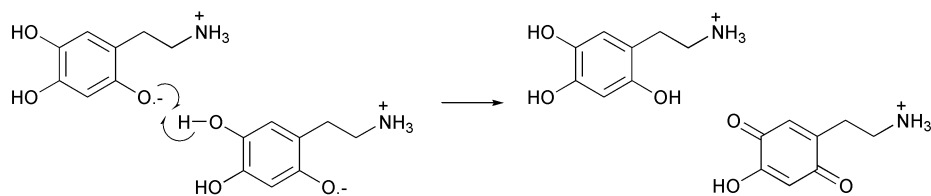
The extent of this second-order contribution depends upon both the relative concentration of iron(III) and on the pH. At low pH and at higher iron concentrations the curve exhibits first-order behaviour over the measured time-scale. At higher pHs and lower iron concentrations it is mainly second-order.

It is known that semiquinones can undergo the following disproportionation equilibrium<sup>8</sup> (where sq = semiquinone; Q = quinone; L = fully reduced molecule), eqn. (16).



This second-order contribution could, therefore, be the combination of two *p*-semiquinones to produce  $pQ$  and a 6-hydroxydopamine, presumably by hydrogen atom abstraction (see Scheme 2). This is supported by the observation that  $pQ$  and  $Q^-$  are still being formed long after the formation of  $oQ$  has stopped, (which implies that all the iron(III) has been consumed). One can also conclude from this that the *p*-semiquinone is particularly stable in contrast to the *o*-semiquinone, which reacts immediately with another iron(III). Further evidence for the existence of this reaction is provided by the fact that, at very low concentrations of iron, an induction curve is observed followed by second-order kinetics (see Fig. 7). In other words the *p*-semiquinone is initially formed very rapidly but because of a lack of iron(III),  $pQ$  is subsequently formed exclusively by means of the disproportionation reaction given in Scheme 2.

The proposed reaction scheme is given in eqns. (17)–(19).



Scheme 2 Plausible reaction scheme for the disproportionation of the *p*-semiquinone.

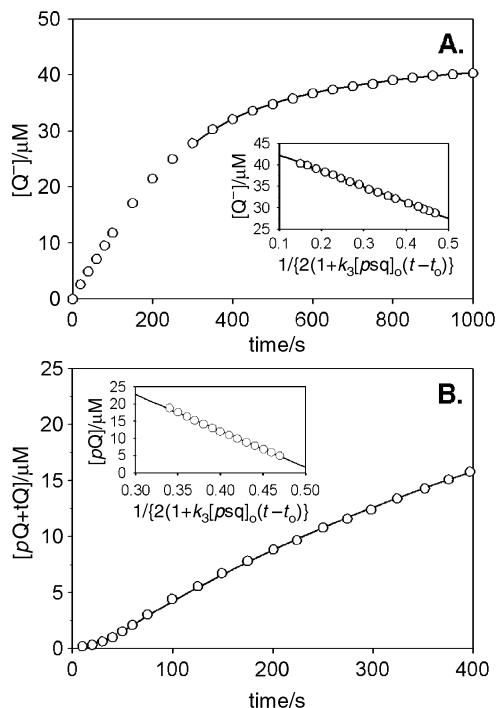
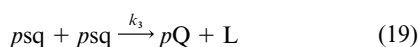
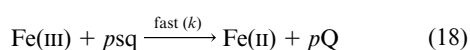
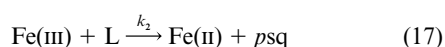


Fig. 7 A. Second-order contribution to the rate of formation of  $Q^-$  corresponding to disproportionation of the semiquinone. ( $[L] = 0.662$  mM;  $[Fe]_{\text{added}} = 91.2$   $\mu\text{M}$ ;  $\text{pH} = 5.00$ .) B. Plot showing induction period followed by second-order kinetics for low iron of ( $pQ + tQ$ ). ( $[L] = 0.311$  mM;  $[Fe]_{\text{added}} = 2.05$   $\mu\text{M}$ ;  $\text{pH} = 0.98$ .) (The derivation of the theoretical curves is given later in the text. The number of data points has been reduced from 1000 for clarity.)



From this the rate equations [eqns. (20)–(23)] can be obtained.

$$-\frac{d[\text{Fe(III)}]}{dt} = [\text{Fe(III)}]\{k_2[L] + k[psq]\} = \frac{d[\text{Fe(II)}]}{dt} \quad (20)$$

$$-\frac{d[L]}{dt} = k_2[\text{Fe(III)}][L] - \frac{1}{2}k_3[psq]^2 \quad (21)$$

$$\frac{d[psq]}{dt} = k_2[\text{Fe(III)}][L] - k[\text{Fe(III)}][psq] - k_3[psq]^2 \quad (22)$$

$$\frac{d[pQ]}{dt} = k[\text{Fe(III)}][psq] - \frac{1}{2}k_3[psq]^2 \quad (23)$$

Towards the end of the reaction ( $t = t_0$ ) all the iron has been consumed (*i.e.*  $[\text{Fe(III)}] \rightarrow 0$ ) and the semi-quinone ( $psq$ ) has built up to a concentration  $[psq]_0$ , eqn. (24). This can be rearranged

$$\frac{d[psq]}{dt} = -k_3[psq]^2 \quad (24)$$

and integrated from  $[psq]_0$  to  $[psq]$  and  $t_0$  to  $t$  to give eqns. (25)–(27). This is then inserted into the rate equation and the

$$\int_{[psq]_0}^{[psq]} \frac{d[psq]}{[psq]^2} = -k_3 \int_{t_0}^t dt \quad (25)$$

$$\frac{1}{[psq]} - \frac{1}{[psq]_0} = k_3(t - t_0) \quad (26)$$

$$[psq] = \frac{[psq]_0}{\{1 + k_3[psq]_0(t - t_0)\}} \quad (27)$$

$$\int_{[pQ]_0}^{[pQ]} d[pQ] = \frac{k_3[psq]_0^2}{2} \int_{t_0}^t \frac{dt}{\{1 + k_3[psq]_0(t - t_0)\}^2} \quad (28)$$

resulting expression integrated to give eqn. (28) which can be rewritten as eqn. (29) or (30).

$$[pQ] - [pQ]_0 = \frac{k_3[psq]_0^2}{2} \left\{ \frac{1}{k_3[psq]_0} - \frac{1}{k_3[psq]_0\{1 + k_3[psq]_0(t - t_0)\}} \right\} \quad (29)$$

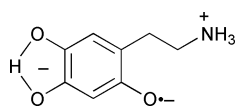
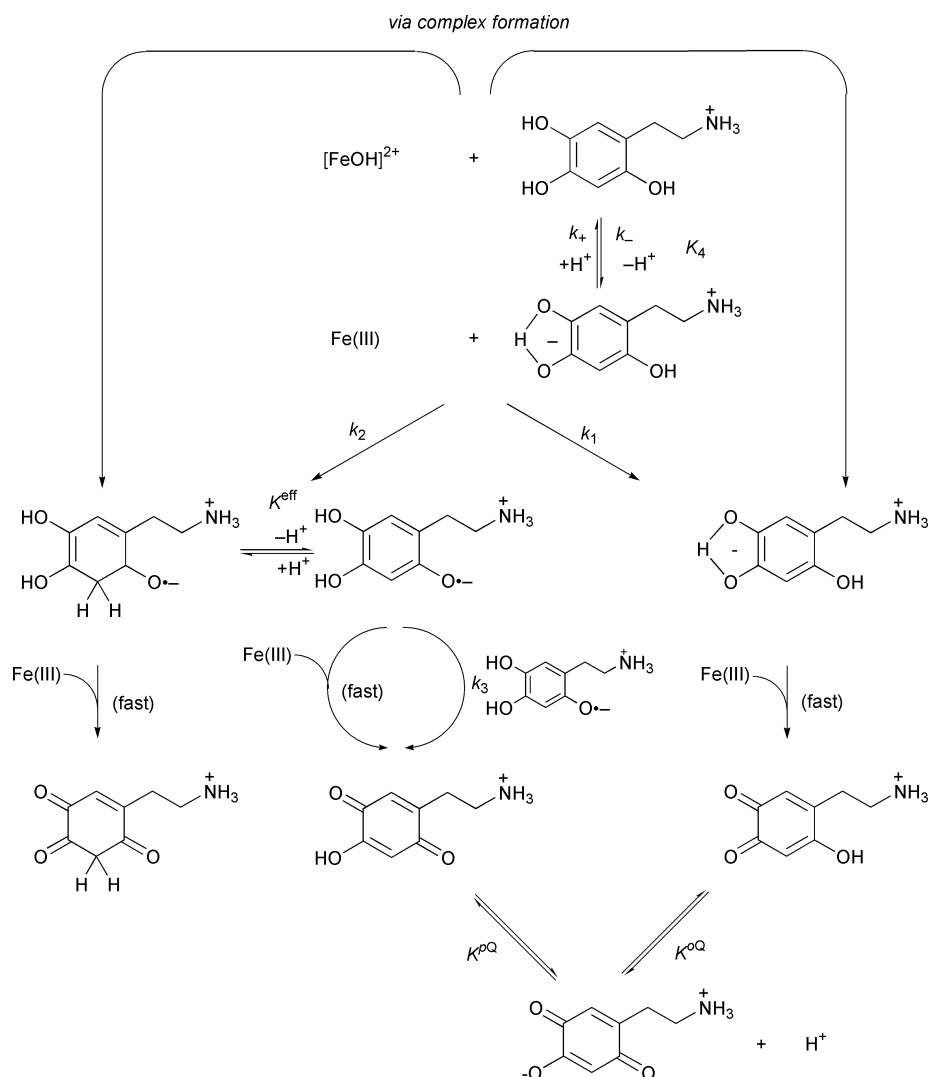
$$[pQ] = \frac{[psq]_0}{2} + [pQ]_0 - \frac{[psq]_0}{2\{1 + k_3[psq]_0(t - t_0)\}} \quad (30)$$

Therefore,  $[pQ]$  was plotted against  $1/2\{1 + k_3[psq]_0(t - t_0)\}$ , and the values of  $k_3$ ,  $t_0$ , and  $[psq]_0$  varied until the best straight line was fitted. (Absorptions were converted to concentrations (*i.e.*  $[pQ]$  or  $[Q^-]$ ) by using the extinction coefficients previously obtained in Part 2.) Note that when  $t_0$  is defined, so also is  $[pQ]_0$ , and the intercept can be used to check that the fit is internally consistent. Furthermore,  $t_0$  was increased until the value for  $k_3$  did not vary any further. That is because as the extent of reaction increased so the assumption that all the iron has been used up is more valid. Therefore only the second-order reaction is taking place. An example of the fit obtainable is given in the insets in Fig. 7.

Values for the second-order rate constant have been obtained over a wide range of pHs (at higher pHs the formation of  $Q^-$  can be followed) and these are shown in Fig. 8.

The observed rate constant is seen to be relatively constant but then starts to rise slowly above a pH of about 6, consistent with a log  $K$  value of 6.8 although this value is, of course, only approximate. Although the two protonated semiquinones react fairly slowly at low pH, when the semiquinone deprotonates the reaction rate increases rapidly, presumably because hydrogen atom abstraction is facilitated. The log  $K$  value of about 6.8 therefore refers to the deprotonation of the semiquinone and it is significant that it lies between that of the 6-hydroxydopamine (log  $K = 8.88$ ) and the quinone (log  $K = 4.13$ ).

This deprotonated *p*-semiquinone will presumably have the structure shown below.



There are two possible ways to explain the enhanced reactivity of this species. Either the hydrogen bridge changes the reactivity of the  $-O^{\bullet-}$  group or, conceivably, the bridging proton could be more readily removed as an atom. However, this latter explanation would require the interaction of two negatively charged centres.

### Other approaches

During the course of this work, two other lines of approach to the problem of solving the second-order reaction were used with some limited success.

Firstly, the scheme (assuming  $oQ$  was not formed) was modelled using the non-linear fitting program Scientist from Micromath. Although this succeeded in producing curves of the correct general form observed (*i.e.* very similar to the curves illustrated in Figs. 2 and 7) the program (or computer) could not cope with the numerical solutions of the differential equations required in order to fit actual data with theory.

Secondly, it was seen that Chien<sup>9</sup> and later Pearson *et al.*<sup>10</sup> had solved some of these very complicated reaction schemes by the use of Bessel functions. Again this line of approach had a certain success but to fit the overall scheme proved too difficult because the parallel reaction to form the *o*-quinone cannot be ignored and, unfortunately, a scheme including this cannot be

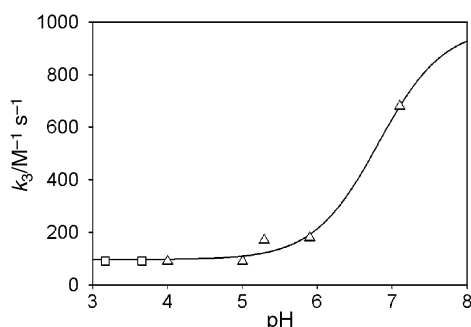


**Fig. 8** pH dependence of the second-order rate constants for the disproportionation of the semiquinones. The superimposed curve assumes a  $\log K$  value of 6.8 and a maximum rate of  $950 M^{-1} s^{-1}$ . □ =  $pQ$ , △ =  $Q^-$ .

solved analytically. Therefore, the method finally adopted was that outlined above, despite the fact that it was only possible to deal with either end of the reaction. Even this fails as far as initial rate determinations are concerned when the iron concentrations are low and a long induction period occurs (Fig. 7).

### The overall reaction scheme

At low pH it has been shown in Part 2 that  $tQ$  is the main component of the 265 nm band. At these pHs there is little sign of a second-order reaction occurring indicating that this, like  $oQ$ , is formed by rapid attack of a second iron(III) on the semiquinone.

**Table 1** The rate constants obtained (see Scheme 3)

$k_{-1}/s^{-1}$	$k_{+1}/M^{-1}s^{-1}$	$k_1/M^{-1}s^{-1}$	$k_2/M^{-1}s^{-1}$	$k_3/M^{-1}s^{-1}$
550	$4.2 \times 10^{11}$	$4.6 \times 10^8$	$8.8 \times 10^8$	pH dependent

The problem of a pH dependence on the amount of *p*Q formed at low pH has been solved by allowing a protonation equilibrium between the triketo- and *p*-semiquinones. This was necessary because there is no equilibrium between the quinones themselves over the time-scales employed. This was established by NMR studies (see Part 1 in this series) and discussed fully when drawing up the speciation diagram in Part 2. The completed reaction scheme incorporating all these features is depicted in Scheme 3.

The rate of disappearance of iron(III),  $k_{\text{rxn}} = (k_1 + k_2)$ , has been calculated to be  $1.34 \pm 0.05 \times 10^9 M^{-1} s^{-1}$ . It has now been established, by NMR and the speciation investigations, that the ratio of the sum of *t*Q and *p*Q produced at low pH to *o*Q is 1.94. It therefore follows that from this that  $k_2 = 1.94k_1$ . Hence the rate of formation of *o*Q from the reaction of all species of iron(III) with the deprotonated 6-hydroxydopamine,  $k_1$ , is  $4.6 \times 10^8 M^{-1} s^{-1}$  and that for *p*Q,  $k_2 = 8.8 \times 10^8 M^{-1} s^{-1}$  (Table 1).

### Biological implications and conclusions

It can be clearly seen that 6-hydroxydopamine reacts with iron(III) in an extremely complicated way. The mechanism is not completely unique, however, and comparisons with the other catecholamines, and noradrenaline in particular, can be drawn. Dopa, dopamine, and adrenaline form catecholate complexes which undergo internal electron transfer.<sup>2,3</sup> Noradrenaline,<sup>4</sup> on the other hand, was found to react by parallel inner- and outer-sphere mechanisms but mainly *via* complex formation. A relation between reduction potential and reactivity should be possible but the redox potentials are difficult to measure and almost certainly the one-electron redox potentials are more important and as yet unmeasured.

The ability of 6-hydroxydopamine to react *via* an outer-sphere mechanism allows very fast rates to be achieved. This reaction *via* direct electron transfer (“outer-sphere” electron transfer) means that 6-hydroxydopamine can react at all pHs with iron(III), whereas dopamine forms bis- and tris-complexes at physiological pHs that are stable towards electron exchange. This seems to be an important part of its chemistry and maybe explains why it is so dangerous to biological systems. The

addition of a third hydroxy group to dopamine radically alters its properties explaining why, alone among the catecholamines, 6-hydroxydopamine is able to interact with the iron(III) stored in ferritin. (Our investigations into this reaction will be published elsewhere.)

### Acknowledgements

The authors wish to thank the “Fonds zur Förderung der wissenschaftlichen Forschung” (FWF) (Project No. 11218-CHE), and the Austrian Federal Ministry of Science and Transport (Project No. GZ 70.023/2-Pr/4/97). This project was also supported by the “Österreichische Nationalbank” (Project No. 5556). We would further like to thankfully acknowledge the support of this project *via* the EU COST project D8 (Chemistry of Metals in Medicine) and the TMR project (TOSS) supported by the European Community under the Contract number ERB-FMRX-CT98-0199.

### References

- 1 W. Linert, E. Herlinger, R. F. Jameson, E. Kienzl, K. Jellinger and M. B. H. Youdim, *Biochem. Biophys. Acta*, 1996, **1316**, 160.
- 2 U. El-Ayaan, E. Herlinger, R. F. Jameson and W. Linert, *J. Chem. Soc., Dalton Trans.*, 1997, 2813.
- 3 W. Linert, R. F. Jameson and E. Herlinger, *Inorg. Chim. Acta*, 1991, **187**, 239; W. Linert, E. Herlinger and R. F. Jameson, *J. Chem. Soc., Perkin Trans. 2*, 1993, 2435.
- 4 U. El-Ayaan, R. F. Jameson and W. Linert, *J. Chem. Soc., Dalton Trans.*, 1998, 1315.
- 5 J. E. Gorton, PhD Thesis, University of St. Andrews, Scotland, 1968.
- 6 P. W. Atkins, *Physical Chemistry*, 4th edn., Oxford University Press, Oxford, 1990, p. 860.
- 7 H. Strehlow, *Rapid Reactions in Solution*, VCH, Weinheim, 1992, p. 108; D. A. McQuarrie and J. D. Simon, *Physical Chemistry, A Molecular Approach*, University Science Books, Sausalito, California, 1997, p. 1070.
- 8 J. K. Dohrmann and B. Bergmann, *J. Phys. Chem.*, 1995, **99**, 1218; A. E. Alegria, M. López and N. Guevara, *J. Chem. Soc., Faraday Trans.*, 1996, **92**, 4965; V. A. Roginsky, L. M. Pisarenko, W. Bors, C. Michel and M. Saran, *J. Chem. Soc., Faraday Trans.*, 1998, **94**, 13, 1835; V. A. Roginsky, L. M. Pisarenko, W. Bors and C. Michel, *J. Chem. Soc., Perkin Trans. 2*, 1999, 871.
- 9 J.-Y. Chien, *J. Am. Chem. Soc.*, 1948, **70**, 2256.
- 10 R. G. Pearson, L. C. King and S. H. Langer, *J. Am. Chem. Soc.*, 1951, **73**, 4149.
- 11 Part 1. G. N. L. Jameson, A. B. Kudryarstev and W. Linert, *J. Chem. Soc., Perkin Trans. 2*, 2001 (DOI: 10.1039/b007912j).
- 12 Part 2. G. N. L. Jameson and W. Linert, *J. Chem. Soc., Perkin Trans. 2*, 2001 (DOI: 10.1039/b007162p).